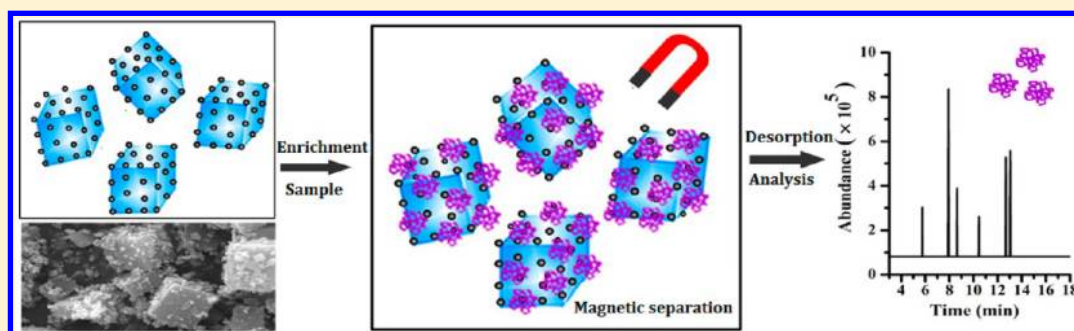


Chemical Bonding Approach for Fabrication of Hybrid Magnetic Metal–Organic Framework-5: High Efficient Adsorbents for Magnetic Enrichment of Trace Analytes

Yuling Hu,* Zelin Huang, Jia Liao, and Gongke Li*

School of Chemistry and Chemical Engineering, Sun Yat-sen University, Guangzhou, 510275, China

S Supporting Information



ABSTRACT: A facile and efficient strategy about the synthesis of a novel kind of hybrid magnetic metal–organic framework (MOF)-5 via chemical bonding assembly was reported. The covalent bonding established between the amino functionalized Fe_3O_4 nanoparticles and the surface of the metal organic framework improved the chemical stability and structure uniformity of the hybrid microcrystals. Combination of MOF-5 with Fe_3O_4 nanoparticles allows for facile withdrawal of the porous materials by magnetic decantation. The powder X-ray diffraction patterns of the hybrid magnetic MOF-5 showed the structure of the metal organic framework was not disturbed with the decoration of magnetic nanoparticles. The as-synthesized materials combine the favorable attributes of both magnetic characteristics of Fe_3O_4 nanoparticles and high porosity of metal organic framework, making them excellent candidates as adsorbents for magnetic enrichment of trace analytes. Their potential applications were explored by preconcentrating polycyclic aromatic hydrocarbons and gibberellic acids from environmental, food, and plant samples prior to gas chromatography–mass spectrometry (GC/MS) and liquid chromatography–tandem mass spectrometry (LC-MS/MS), respectively. The results showed that the magnetic MOF-5 exhibited superior enrichment capacity for both of these nonpolar and polar analytes. The method demonstrated good precision (relative standard deviations (RSDs) of 1.7–9.7%), low detection limits ($0.91\text{--}1.96\text{ ng}\cdot\text{L}^{-1}$ for polycyclic aromatic hydrocarbons and $0.006\text{--}0.08\text{ }\mu\text{g}\text{ L}^{-1}$ for gibberellic acid), and good linearity (correlation coefficients higher than 0.9949). The RSDs of batch-to-batch extraction were 2.9–11.2%. The magnetic MOF-5 was robust enough for repeatable use without damage of extraction performance.

Porous metal–organic frameworks (MOFs) are highly ordered crystalline materials prepared by self-assembly of metal ions with organic linkers to yield low density network structures of diverse topology.¹ MOFs have attracted considerable attention over the past decade.^{2–6} Their unique characteristics also make MOFs promising for diverse applications in analytical chemistry, for instance, as sorbents for sampling,^{7,8} solid-phase extraction,^{9,10} solid-phase micro-extraction,^{11,12} and as stationary phases for chromatography.^{13,14}

Recently, multifunctional materials have been a topic of growing interest as they involve diverse characteristics in one material.^{15,16} In this field, chemically synthesized magnetic composites are of particular interest for their unique magnetic properties. Magnetic composites based on graphene, carbon nanotubes have been successfully investigated.^{17,18} Considering the superior properties of MOFs and their successful development in a wide range of research fields, the design

and synthesis of magnetic MOFs are especially desirable. Magnetization of MOFs can be implemented by incorporating magnetic carriers such as paramagnetic metals or open-shell organic ligands.¹⁹ However, these intrinsic magnetic properties of MOFs derived from the central ions and framework are usually limited and not suitable for magnetic separation. Another approach is the functionalization of MOFs with superparamagnetic iron oxide nanoparticles. Nevertheless, the synthesis is currently subject to a challenging goal, and so far, there are limited reports,^{20,21} for instance, the preparation of the composites of Fe_3O_4 nanoparticles with MOFs by nanoparticle surface modification and the formation of core–shell structure by a step-by-step assembly strategy. Owing to

Received: April 20, 2013

Accepted: June 13, 2013

Published: June 13, 2013

the convenience of retrieval of adsorbents from sample matrix, magnetization of MOFs for applications to sample preparation has sparked great excitement. Recently, Yan and co-workers²² has reported a simple method by physically mixing MIL-101 and silica-coated Fe₃O₄ microparticles under sonication for rapid magnetic solid-phase extraction of polycyclic aromatic hydrocarbons (PAHs) in environmental water samples. The results with large enrichment factor suggest that the method of magnetic separation with MOFs is attractive for its rapidness and efficient extraction. However, loading of MOFs with magnetic nanoparticles through chemical bonding would endow the resultant materials with higher chemical stability, durable magnetism, and better reproducibility. Looking at the diverse surface chemistry of MOFs, much research has been done concerning the surface characterization,^{23,24} functionalization of MOF cavity,^{25–28} postsynthesis modification^{29,30} and surface chemistry at liquid–solid interface.³¹ Recently, Park and co-workers³² demonstrated the bioconjugation of functional proteins onto the surface of MOFs, in which they proved that a certain amount of the carboxyl groups are exposed on the surface of MOFs which can be activated for chemical reactions. This research sparked us to efficiently magnetize the MOFs through surface modification.

Herein, we describe a novel scheme to fabricate the magnetic metal organic framework decorated with Fe₃O₄ nanoparticles via chemical bonding assembly, which was expected to endow the composite with desirable stability, durability, and repeatability. The Fe₃O₄ nanoparticles was first functionalized with amino groups and then chemically bonded to the surface of MOF-5 crystals, which has a chemical formula of Zn₄O(BDC)₃ (BDC = 1,4-benzenedicarboxylate). The obtained hybrid magnetic MOF-5 was applied to magnetic separation and enrichment of polycyclic aromatic hydrocarbons (PAHs) and gibberellic acid (GAs) from environmental, food, and plant samples, respectively. PAHs are selected as the analytes due to their toxic, mutagenic, and carcinogenic characteristics. GAs are important plant hormones that greatly influence plant developmental processes including stem elongation, germination, dormancy, flowering, and sex expression. The determination of PAHs and GAs in environmental and biological samples is a major challenge for their ultra trace concentration levels, usually at ng g⁻¹ and even pg g⁻¹ levels. To the best of our knowledge, this is the first example to create robust magnetic MOFs with covalent bonding linkage for magnetic separation and enrichment.

■ EXPERIMENTAL SECTION

Reagents and Instruments. Zinc acetate, ferric chloride, and ferrous sulfate were all of analytical grade and bought from Shenyang Chemical Reagent Factory (Shenyang, China). *N,N'*-Dimethylformamide (DMF) and tetraethylorthosilicate (TEOS) of analytical grade were obtained from Tianjing Chemical Reagent Factory (Tianjing, China). Terephthalic acid (≥99%) and 3-aminopropyl triethoxysilane (APTES, ≥98%) were purchased from Aladdin Chemistry. Naphthalene (NAP, 98.8%), acenaphthene (ANE, 99%), fluorene (FLU, 98%), phenanthrene (PHE, 99%), fluoranthene (FLA, 98%), and pyrene (PYR, 99%) were purchased from Chem. Service (America). GA3 (purity ≥98%) was obtained from Dingguo Bio-Technology Co. Ltd. (Beijing, China). GA1 (purity ≥98%) and the mixed standard of GA4 and GA7 (*m:m* = 7:3, purity ≥98%) were obtained from Bio. Basic Inc. (Canada). A stock solution of GAs was prepared at a concentration of 100

mg·L⁻¹ in methanol and stored at 4 °C in the dark. The working standard solution was prepared by appropriate dilution of the stock standard solution with methanol to obtain a desired concentration. All other reagents were at least of analytical grade.

Scanning electron microscopy (SEM) images were recorded on an S-4300 SEM instrument (HITACHI, Japan). Transmission electron microscopic (TEM) characterization was performed on a PHILIPS TECNAI 10 TEM instrument (Philips, Netherlands). X-ray diffractometry (XRD) was carried out using a RIGAKU diffractometer. X-ray photoelectron spectroscopy (XPS) experiments were performed on an ESCA LAB 250 XPS instrument. Infrared absorption spectra were conducted on a NICOLET AVATAR 330 Fourier transform infrared (FT-IR) spectrometer. A thermogravimetric (TG) analyzer (Netzsch-209, Bavaria, Germany) was used to evaluate the thermal stability. The magnetic property of the hybrid material was characterized by a SQUID-based magnetometer from Quantum Design (San Diego, CA).

Preparation of the Amino Functionalized Fe₃O₄ Nanoparticles. First, Fe₃O₄ nanoparticles with the diameter of 30–50 nm were prepared by microwave synthesis according to the previous work;³³ for details, please see the Supporting Information. Then, ammonia solution (30 wt %) was dropped into a mixed solution of water and ethanol (1:4, v:v) containing Fe₃O₄ nanoparticles under stirring. Tetraethylorthosilicate was added and maintained for 24 h at 40 °C. The resultant nanoparticles were collected, washed with ethanol and dried at 150 °C under vacuum. Then, the obtained products were reacted with 3-aminopropyl triethoxysilane to obtain amino functionalized Fe₃O₄ nanoparticles under continuous agitation for 7 h at room temperature.

Synthesis of the Hybrid Magnetic MOF-5. MOF-5 was synthesized according to Yaghi's report³⁴ with minor modifications. In brief, terephthalic acid (0.5065 g, 3.05 mmol) was dissolved in 40 mL of *N,N'*-dimethylformamide. Zn(OAc)₂·2H₂O (1.699 g, 7.74 mmol) was dissolved in 50 mL of *N,N'*-dimethylformamide. The zinc salt solution was dropped into the solution of terephthalic acid with stirring over 15 min. White precipitates were formed immediately. Then, 0.80 g of amino functionalized Fe₃O₄ nanoparticles was immediately added under ultrasound and maintained for 30 min to ensure uniform dispersion. The mixture was transferred into the autoclave, sealed, and maintained for 10 h at 120 °C. After being cooled down to room temperature, the precipitate was collected by a magnet and washed with *N,N'*-dimethylformamide. For comparison, the bare Fe₃O₄ nanoparticles were physically mixed with MOF-5 under the same condition described above.

Procedure of Magnetic Separation and Enrichment. For extraction of GAs, 30 mg of the hybrid magnetic MOF-5 was added to 10 mL of standard solution or sample dissolved in *n*-hexane in a conical flask. The solution was first immersed into an ultrasonic bath for 30 s and then shaken on a rotator for a certain period. The hybrid magnetic MOF-5 was then collected by applying a magnet to the outer wall of the vial and eluted with 1.0 mL of acetonitrile containing 1% formic acid under ultrasound. The supernatant was evaporated under a gentle nitrogen stream. Finally, the analytes were redissolved in 100 μL of formic acid–water (0.1%, v:v), followed by liquid chromatography-tandem mass spectrometry (LC-MS/MS) analysis. The magnetic separation and enrichment procedure for PAHs was similar to that of GAs. The magnetic MOF-5 (50

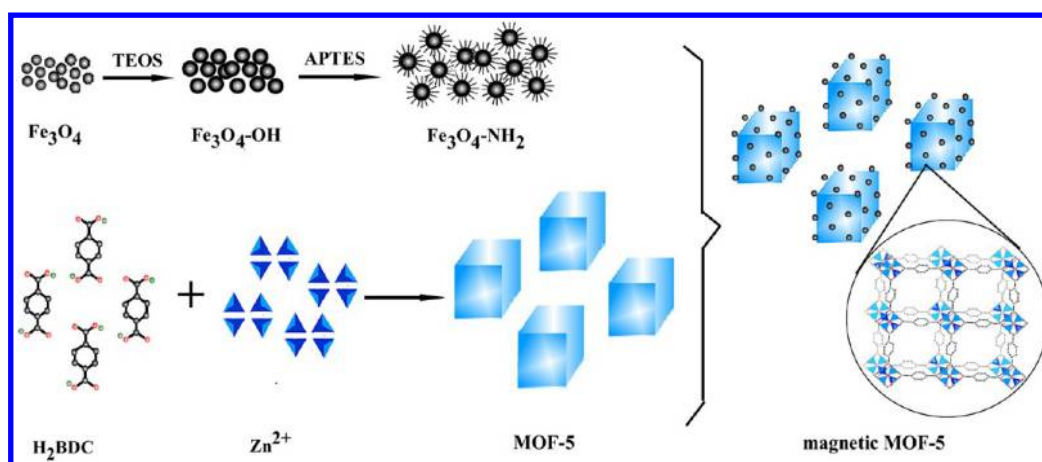


Figure 1. Schematic of the fabrication processes of the hybrid magnetic MOF-5.

mg) was added to 25 mL of PAH solutions dissolved in *n*-hexane for extraction. Desorption was performed with 0.25 mL of acetone.

Chromatographic Analysis. A Shimadzu 2010 gas chromatography–mass spectrometry (GC/MS) system was used for analysis of the PAHs. A DB-5 MS (Agilent Scientific, USA) capillary column (30 m length \times 0.25 mm i.d. \times 0.25 μ m film thickness) was used for the chromatographic separation. The analysis of GAs was carried out by a Shimadzu LC-MS/MS 8030 (Shimadzu, Japan). A reversed-phase column of C_{18} (75 mm \times 3.0 mm i.d., 5 μ m) (Shimadzu, Japan) was used. For more details of chromatographic conditions, please see the Supporting Information.

Samples. For the analysis of PAHs, a soil sample was collected from a petrol station (Guangzhou, China). Seaweed and fish samples were collected from local market. For GAs, seeds of buckwheat, mung bean, and wheat were soaked in water for germination in a growth chamber. After growing for 1 week, the height of the plant was 5–8 cm, and then, the whole plant except the root was harvested and grounded. The sample preparation procedures prior to magnetic enrichment were described in the Supporting Information.

RESULTS AND DISCUSSION

Fabrication of the Hybrid Magnetic MOF-5. The framework of MOF-5 is based on the coordination interaction between the carboxyl group of terephthalic acid and the Zn^{2+} of $Zn(OAc)_2 \cdot 2H_2O$. Either pendent ZnO_4 nodes or carboxyl groups should occupy the surface of the frameworks. Recently Park and co-workers³² confirmed an assumption that a certain amount of the carboxyl groups are exposed on the crystalline surface and can be conjugated with other compounds via chemical interaction. Accordingly, in our research, the Fe_3O_4 nanoparticles were first functionalized with amino groups, which can form covalent bonding with the pendent linking groups of the organic linkers of carboxyl groups exposed on the surface of MOF-5 (Figure 1). The content of Fe_3O_4 nanoparticles was optimized to ensure sufficient magnetization of the MOFs and less unbound Fe_3O_4 nanoparticles. The surface modification procedure for Fe_3O_4 nanoparticles was essential to create binding sites or reactive centers. If the Fe_3O_4 nanoparticles were not surface functionalized, the as-synthesized material was simply a physical blending of the two components, which led to obvious hierarchy in the resultant solution (Figure S1, Supporting Information), indicating that

the Fe_3O_4 nanoparticles and MOF-5 were partially separated from each other. In fact, milky fine particles would be continuously discharged from the material by physical blending of Fe_3O_4 and MOF-5 under ultrasonic cleaning, which indicated the gradual loss of MOF-5. As a result, the extraction ability of the physical mixture of Fe_3O_4 and MOF-5 gradually decreased after repeated use because of its lower stability (Figure 2). Compared with the physical blending method, the

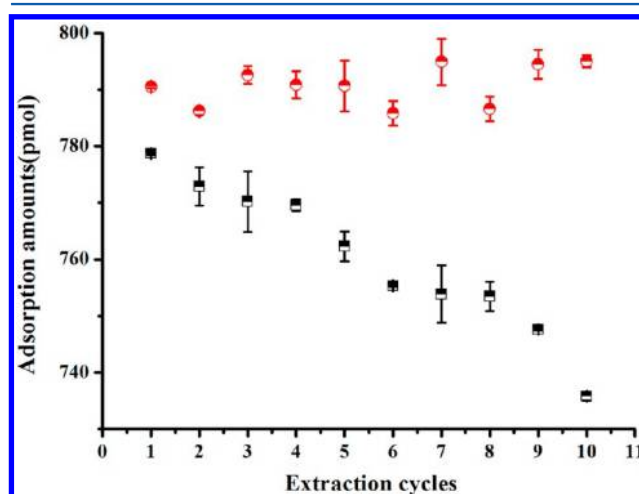


Figure 2. Stability of the magnetic MOF-5 which was fabricated by physical blending (■) or the chemical bonding strategy (red ●).

chemical bonding approach improved the chemical stability, uniformity, and permanent magnetism of the composites. The proposed preparation method was reproducible, and the resultant hybrid magnetic MOF-5 was stable enough to be applied in replicate at least for 100 extraction cycles.

Characterization of the Hybrid Magnetic MOF-5. The XRD patterns of the parent materials (MOF-5, $NH_2-Fe_3O_4$) and the hybrid materials are presented in Figure 3A. The main diffraction peaks at low angles, $2\theta = 6.9^\circ$ ($\langle 200 \rangle$ plane, $d = 12.8$ Å) and 9.7° ($\langle 220 \rangle$ plane, $d = 9.1$ Å) are indicative of the modular arrangement of the MOF-5 cubic lattice.³⁵ Most peaks from MOF-5 are preserved in the XRD patterns of the as-synthesized hybrid magnetic MOF-5 and are in good agreement with that reported by Yaghi.³⁴ This suggests that attachment of Fe_3O_4 nanoparticles on MOF-5 did not destroy the crystal structure of the framework. In addition, the presence

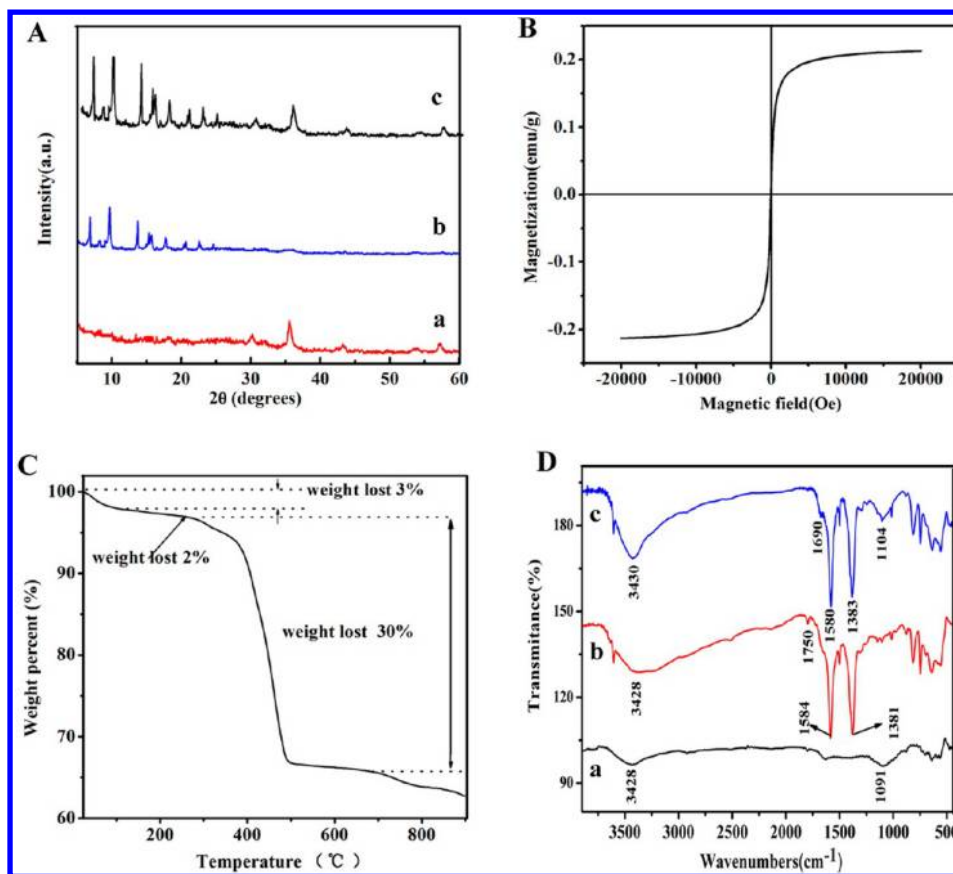


Figure 3. Characterization of the hybrid magnetic MOF-5. (A) XRD pattern of the NH₂-Fe₃O₄ (a), MOF-5 (b), and the as-synthesized hybrid magnetic MOF-5 (c); (B) magnetization curve and (C) TG curve of the as-synthesized hybrid magnetic MOF-5; (D) FT-IR spectra of the NH₂-Fe₃O₄ (a), MOF-5 (b), and the hybrid magnetic MOF-5 (c).

of Fe₃O₄ nanoparticles allows for facile separation of the hybrid material from sample matrix by applying a magnetic field. The magnetization curve of the hybrid material exhibits superparamagnetic characteristics (Figure 3B). The saturation magnetization values were measured to be 0.22 emu·g⁻¹, which is not very strong owing to the surface magnetization instead of the bulk incorporation. However, the magnetism of the resultant hybrid material is sufficient to meet the requirement for magnetic separation of the solid material from liquid matrix. Additionally, the surface modification strategy prevents the blockage of the inner pore in the framework. The TGA data revealed that the hybrid magnetic MOF-5 was stable up to 300 °C (Figure 3C). The FT-IR spectra illustrated in Figure 3D revealed the chemical structure of the material. The stretching vibration of C=O (–COOH) at 1750 cm⁻¹, which is the evidence of the presence of free carboxyl in MOF-5, disappeared in the FT-IR spectra of the hybrid magnetic MOF-5, indicating chemical reaction occurred on the basis of carboxylate groups being exposed on the surface of MOF-5. The new weak signal of 1690 cm⁻¹ (acylamide I band) indicated the formation of para-acylamino. The bending vibration of the N–H bond of para-acylamino (acylamide II band) was not observed, probably because the band was so weak and near the asymmetric stretch of the coordinated carboxylate groups at 1584 cm⁻¹ in MOF-5 and thus would be easily covered by the strong band.^{36,37}

In order to further demonstrate the chemistry of the as-synthesized hybrid magnetic MOF-5, the XPS was evaluated (Figure S2, Supporting Information). The oxygen-, zinc-,

nitrogen-, and iron-related peaks are detected in the XPS spectra obtained for the magnetic MOF-5. Deconvolution of the N1s peak shows the presence of both –NH₂ at 401.9 eV and –C(O)NH at 399.9 eV, indicating the formation of amide bond. Similarly, the deconvolution of the O1s peak also suggests that the formation of hybrid magnetic MOF-5 was grown via the chemical interaction between the two components.^{38,39}

To gain a better understanding of the morphological structure of the as-synthesized hybrid magnetic MOF-5, the samples were also characterized using SEM and TEM (Figure 4). The SEM images clearly demonstrate that the surface of MOF-5 has been decorated with clustered Fe₃O₄ nanoparticles, which is direct evidence of successful magnetization of MOF-5 with Fe₃O₄ nanoparticles. The as-synthesized material is a real hybrid composite rather than a physical mixture of two separate components of MOF-5 and Fe₃O₄. Some bare Fe₃O₄ nanoparticles unbound to MOF-5 are also observed because of incomplete reaction. Generally, the binding of Fe₃O₄ nanoparticles has no influence on the cubical crystal of the MOF-5.

Adsorption Characteristics of the Hybrid Magnetic MOF-5. The research about the adsorption characteristics of the hybrid magnetic MOF-5 for organic analytes is critical to explore their potential applications. Considering the abundant phenyl rings as bridges throughout the bulk framework of the magnetic MOF-5, a series of organic compounds, including nonpolar analytes (PAHs) and polar analytes (phenylamine, phenethylol, phenol, and benzoic acid) were selected as model

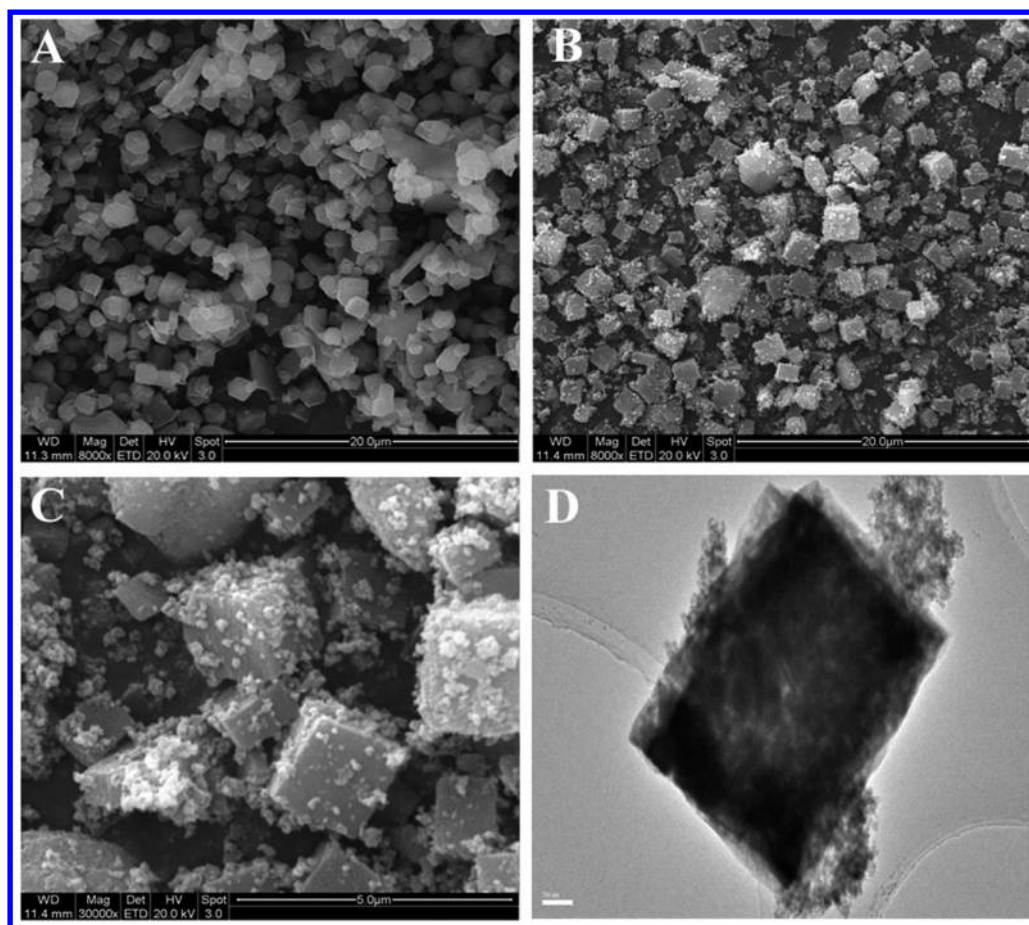








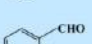
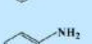



Figure 4. SEM images of the MOF-5 at magnification of 8000-fold (A), the as-synthesized hybrid magnetic MOF-5 at magnification of 8000-fold (B) and 30 000-fold (C), and TEM image of the as-synthesized hybrid magnetic MOF-5 (D).

analyte, and their adsorption affinity on the magnetic MOF-5 was evaluated and shown in Table 1. PAHs are compounds endowed with π - π conjugate structure and would have strong affinity with the magnetic MOF-5 rich in aromatic rings. The adsorption amounts of PAHs increased with an increase of the conjugated double bonds and condensed ring, further indicating the potential main role of the π - π stacking interaction. In contrast, a much lower adsorption amount of decalin was obtained on the hybrid material. With regard to polar aromatic compounds, it appeared that these compounds had much higher adsorption amounts than nonpolar species (e.g., methylbenzene). It was reported that hydrogen bonding between the hydrogen atoms in guest molecules and the oxygen atoms in ZnO_4 of MOF-5 played an important role for adsorption of small molecules, such as water and ammonia.⁴⁰ We suggest that the presence of hydrogen bonding contribute to the interaction between the polar analytes and the adsorbents. The adsorption amounts of benzoic acid was the highest, probably because its stronger ability to form hydrogen bonding with oxygen atoms in ZnO_4 . On the basis of the above results, PAHs and GAs were then selected as the target analytes for investigation of the extraction properties of the hybrid magnetic MOF-5 in real samples. The adsorption isotherms of the magnetic MOF-5 for PAHs and GAs were preliminarily investigated (Figure 5). The high adsorption affinity to PAHs and GAs makes the hybrid material an excellent adsorbent in the following study of real sample analysis.

Application to Analysis of Polycyclic Aromatic Hydrocarbons Followed by GC/MS. PAHs are the widespread ubiquitous contaminants in the environment. Owing to their ultra low concentration, a sensitive method is desired to preconcentrate these analytes prior to detection. The PAHs with highly delocalized π -electrons allow π - π stacking interaction with the aromatic rings of terephthalic acid molecules in the framework of hybrid magnetic MOF-5, which then demonstrates great capability for enrichment of these analytes in combination with the magnetic separation strategy. Different experimental parameters that influence extraction efficiency including extraction time, desorption time, extraction solvent, and desorption solvent were investigated and optimized using 25 mL of standard solution spiked with $100 \text{ ng}\cdot\text{L}^{-1}$ of PAHs (Figure S3, Supporting Information). Extraction time profiles for the six PAHs indicated that the extraction efficiency of most compounds increased as the incubation time increased from 10 to 40 min and remained stable with a further increase of extraction time. All of the PAHs can be desorbed efficiently from the hybrid magnetic MOF-5 within 10 min. Several solvents were tested as extraction or desorption solvents. The results showed that *n*-hexane provided the best extraction efficiency, and acetone provided the best desorption efficiency due to its good dissolving ability for PAHs.

The figures of merit for the magnetic enrichment method combined with GC/MS for determination of PAHs are summarized in Table 2. The six PAHs could be sensitively

Table 1. Adsorption of Different Compounds on the Hybrid Magnetic MOF-5^a

Compounds	Structural formula	Molecular weight	Log K _{OW}	Adsorption amount (nmol·mg ⁻¹)
Decalin		138	4.20	1.74±0.11
Naphthalene		128	3.30	2.66±0.04
Fluorene		166	4.18	2.98±0.09
Phenanthrene		178	4.46	3.35±0.17
Pyrene		202	4.88	3.59±0.18
Methylbenzene		92	2.73	1.63±0.17
Benzaldehyde		106	1.48	2.00±0.18
Phenylamine		93	0.90	3.94±0.49
Phemethylol		108	1.10	4.10±0.36
Phenol		94	1.46	5.00±0.18
Benzoic acid		122	1.87	7.50±0.14

^aK_{ow}: *n*-octanol/water partition coefficients. Data taken from <http://www.syrres.com/what-we-do/databaseforms.aspx?id=386>.

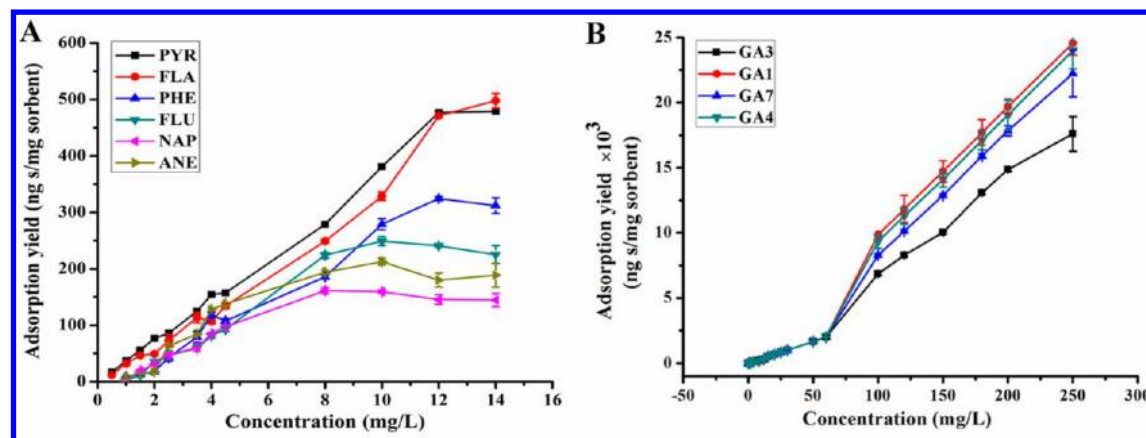


Figure 5. Adsorption yield curves of the hybrid magnetic MOF-5 for adsorption of PAHs (A) in a concentration of 0.5–4.0 mg·L⁻¹ and GAs (B) in a concentration of 0.04–250 mg·L⁻¹.

Table 2. GC/MS Analysis of PAHs in Combination with the Hybrid Magnetic MOF-5

analytes	linear range (ng·L ⁻¹)	detection limits (ng·L ⁻¹)	concentration (ng·g ⁻¹)			recovery ^a (%)			RSD (n = 5) (%)
			soil	seaweed	fish	soil	seaweed	fish	
NAP	5.0–500	1.47	2.11	N.D. ^b	0.27	112.0	106.0	66.4	2.7
ANE	5.0–500	1.14	2.79	N.D.	2.50	76.2	85.8	120.0	1.7
FLU	5.0–500	0.91	0.27	N.D.	0.02	91.5	111.7	76.8	2.3
PHE	5.0–500	1.50	0.72	N.D.	0.10	88.8	80.3	93.6	2.1
PLA	5.0–500	1.96	N.Q. ^c	N.D.	N.Q.	85.5	85.6	94.4	9.7
PYR	5.0–500	1.03	N.Q.	N.D.	N.Q.	98.0	96.3	104.0	7.5

^aSpiked at 2.50 ng·g⁻¹ level of PAHs. ^bN.D., not detected. ^cN.Q., not quantified.

determined with the limits of detection (LODs) in the range of 0.91–1.96 ng·L⁻¹, which were remarkably lower than some previous reports.^{41–44} Satisfactory linearity was obtained with correlation coefficients above 0.9989. The repeatability was measured, and the relative standard deviations (RSDs) were found to be 1.7–9.7% within batch and 2.9–11.2% for batch to batch analysis. These results proved that the as-synthesized hybrid magnetic MOF-5 was quite stable and the fabrication method based on chemical bonding was reproducible.

The method was applied to the analysis of PAHs in soil, seaweed, and fish samples. In order to eliminate the interfering agents from sample matrix, an appropriate sample preparation procedure prior to magnetic enrichment was necessary, and data acquisition of mass spectrum was carried out in the selected ion monitoring (SIM) mode. As shown in Table 2 and Figure 6, four PAHs were detected in the soil sample, ranging

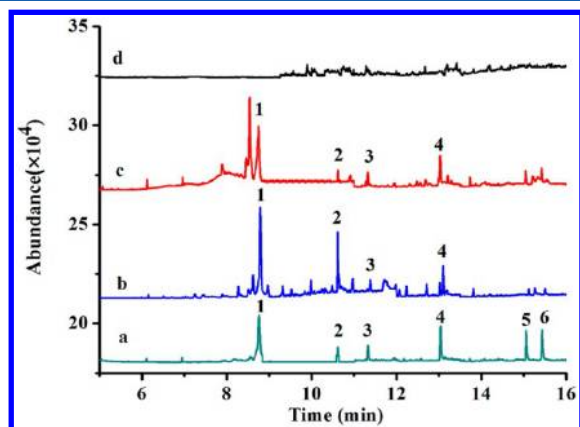


Figure 6. Chromatograms of PAHs for the extracts of 50.0 ng·L⁻¹ standard solution (a), fish sample (b), soil sample (c), and seaweed sample (d) with the hybrid magnetic MOF-5 followed by GC/MS analysis. Peaks: 1 NAP, 2 ANE, 3 FLU, 4 PHE, 5 FLA, and 6 PYR.

from 0.27 to 2.79 ng·L⁻¹. No PAHs were found in the seaweed sample, while four PAHs ranging from 0.02 to 2.50 ng·L⁻¹ were detected in the fish sample (tilapia mossambica). The results are understandable owing to the difference of accumulation effect of PAHs in a different matrix. The nonpolar PAHs are more inclined to accumulate in the lipid matrix during transport. The samples were then spiked with standard solutions of PAHs at 2.50 ng·g⁻¹ to evaluate the recoveries, which ranged from 76.2 to 112.0% for soil, 80.3 to 111.7% for seaweed, and 66.4 to 120.0% for fish samples.

Application to Analysis of Gibberellin Acids in Plant Samples in Combination with LC-MS/MS. In the previous report, most of the analytical applications of MOFs are dealt with compounds of volatile organic compounds and nonpolar compounds. However, the adsorption experiments for different

organic compounds mentioned above indicated even higher adsorption affinity of the hybrid magnetic MOF-5 to polar aromatic compounds. The results from Figure 5 also showed high extraction capacity of the hybrid magnetic MOF-5 to GAs, which might be ascribed to the strong hydrogen bonding interaction between GAs and MOF-5. On the basis of these beneficial results, the as-synthesized magnetic MOF-5 was applied to the analysis of GA3, GA1, GA7, and GA4 in plant samples followed by the LC-MS/MS method.

First, the effect of the extraction and desorption conditions were investigated (Figure S4, Supporting Information). The highest extraction efficiency was obtained with *n*-hexane as the extraction solvent. In order to facilitate efficient desorption of GAs from the hybrid magnetic MOF-5, 1% formic acid was added to acetonitrile which was used as desorption solvent in order to break the hydrogen bonds between GAs and the hybrid magnetic MOF-5. The extraction time and desorption time was 50 and 20 min, respectively.

Then, the characteristic parameters of this novel analytical method were investigated and listed in Table 3. The detection limits of four GAs in the study ranged from 0.006 to 0.08 μg·L⁻¹ based on a signal-to-noise ratio of 3. The proposed method is more sensitive than most of the analytical methods reported previously thanks to highly efficient enrichment of GAs by the hybrid magnetic MOF-5.^{45–47} Satisfactory linearity was obtained with correlation coefficients above 0.9949. The RSDs were achieved in the range of 1.6–9.0% (*n* = 5). As shown in Table 3 and Figure 7, GA3, GA7, and GA4 were detected in buckwheat, ranging from 13.0 to 280.0 ng·g⁻¹, while the concentration of GA1 was below the LODs. GA4 was detected at the concentration of 390.4 and 82.5 ng·g⁻¹ for wheat and mungbean, respectively. Recoveries were obtained by spiking with 200 ng·g⁻¹ of GA1, GA3, and GA7 and 466 ng·g⁻¹ of GA4 and ranged from 71.8 to 127.4%. All the characteristic parameters of the method validated that this method was reliable and sensitive for the analysis of trace GAs in plant samples by magnetic extraction with the hybrid magnetic MOF-5 coupled with LC-MS/MS detection.

CONCLUSIONS

We reported the first example of a simple chemical bonding approach for fabrication of the hybrid magnetic MOF-5 as adsorbents for enrichment of trace analytes in complicated samples. The chemical bonding between the Fe₃O₄ and MOF-5 endows the magnetic MOFs with high chemical stability and desirable durability, which allows the hybrid material cycle to be used without measurable loss of performance. Besides that, the as-synthesized hybrid magnetic MOF-5 offers high enrichment properties and good reproducibility. Its potential application as magnetic adsorbents was tested by enrichment of trace PAHs in soil, seaweed, and fish samples prior to GC/MS analysis, as well as GAs in plant samples prior to LC-MS/MS analysis.

Table 3. LC-MS/MS Analysis of GAs in Combination with the Hybrid Magnetic MOF-5

analytes	linear range (μg·L ⁻¹)	detection limit (μg·L ⁻¹)	concentration (ng·g ⁻¹)			recovery ^a (%)			RSD (<i>n</i> = 5) (%)
			mung bean	wheat	buck wheat	mung bean	wheat	buck wheat	
GA3	0.03–100	0.01	N.D. ^b	N.D.	13.0	97.3	91.7	127.4	1.6
GA1	0.50–100	0.08	N.D.	N.D.	N.D.	102.2	71.8	107.3	3.0
GA4	0.02–60	0.006	82.5	390.4	280.0	104.5	104.7	103.3	9.0
GA7	0.12–140	0.01	N.D.	N.D.	25.0	90.5	93.8	100.3	1.6

^aSpiked with 200 ng·g⁻¹ of GA1,GA3,GA7 and 466 ng·g⁻¹ of GA4. ^bN.D., not detected.

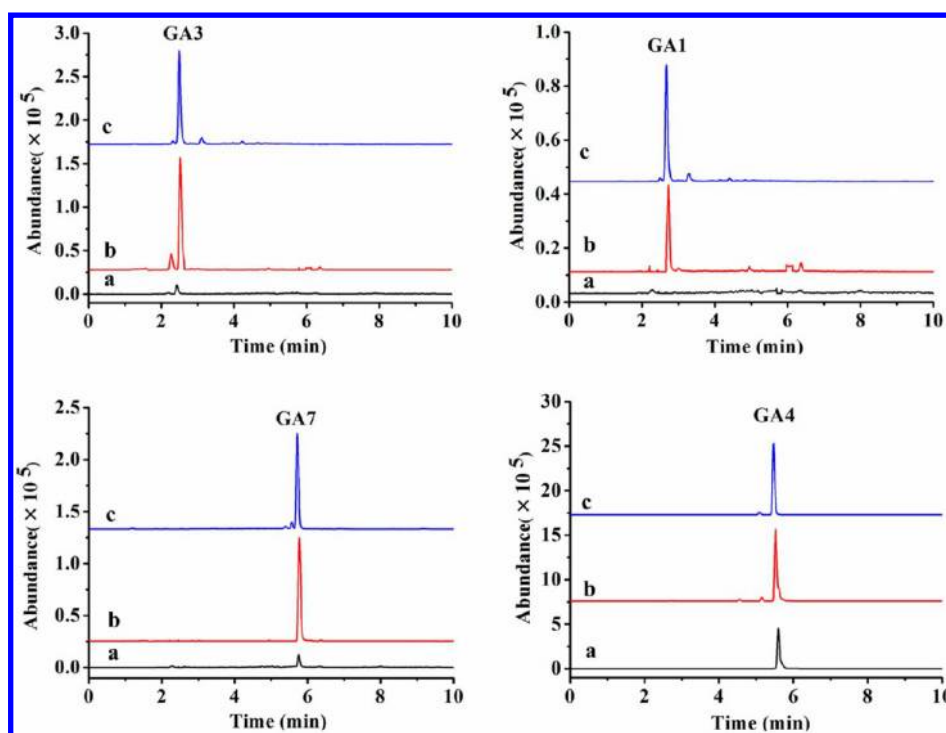


Figure 7. Chromatograms of buckwheat seedling samples obtained by combination of the hybrid magnetic MOF-5 with the LC-MS/MS detection. (a) The buckwheat seedling samples; (b) the buckwheat seedling samples spiked with $200 \text{ ng}\cdot\text{g}^{-1}$ of GA1, GA3, and GA7 and $466 \text{ ng}\cdot\text{g}^{-1}$ of GA4; (c) $20.0 \mu\text{g}\cdot\text{L}^{-1}$ standard solution of GA1, GA3, and GA7 and $46.7 \mu\text{g}\cdot\text{L}^{-1}$ standard solution of GA4.

Considering the diverse structures of MOFs, the chemical bonding approach is promising for fabricating various magnetic MOFs, which combine the favorable attributes of both magnetic properties and unique characteristics of MOFs. It may be possible for the wider application of MOFs owing to the robust combination of magnetic nanoparticles with MOFs and the easy-to-use form.

■ ASSOCIATED CONTENT

📄 Supporting Information

Additional information as noted in text. This material is available free of charge via the Internet at <http://pubs.acs.org>.

■ AUTHOR INFORMATION

Corresponding Author

*Tel.: +86-20-84110922. Fax: +86-20-84115107. E-mail: ceshyl@mail.sysu.edu.cn (Y.H.); cesgkl@mail.sysu.edu.cn (G.L.).

Notes

The authors declare no competing financial interest.

■ ACKNOWLEDGMENTS

This work was supported by the National Natural Science Foundation of China (21277176, 21075140, and 21127008) and Major National Scientific Instrument and Equipment Development Project (2011YQ03012409), respectively. Thank Shimadzu International Trading (Shanghai) Company Limited Guangzhou branch for kindly supporting the LC-MS/MS instrument for experiment.

■ REFERENCES

(1) Bradshaw, D.; Garai, A.; Huo, J. *Chem. Soc. Rev.* **2012**, *41*, 2344–2381.

(2) Yang, S. J.; Choi, J. Y.; Chae, H. K.; Cho, J. H.; Nahm, K. S.; Park, C. R. *Chem. Mater.* **2009**, *21*, 1893–1897.

(3) Alaerts, L.; Kirschhock, C. E. A.; Maes, M.; van der Veen, M. A.; Finsy, V.; Depla, A.; Martens, J. A.; Baron, G. V.; Jacobs, P. A.; Denayer, J. F. M.; De Vos, D. E. *Angew. Chem., Int. Ed.* **2007**, *46*, 4293–4297.

(4) Aguado, S.; Canivet, J.; Farrusseng, D. *J. Mater. Chem.* **2011**, *21*, 7582–7588.

(5) Achmann, S.; Hagen, G.; Kita, J.; Malkowsky, I. M.; Kiener, C.; Moos, R. *Sensors* **2009**, *9*, 1574–1589.

(6) An, J.; Geib, S. J.; Rosi, N. L. *J. Am. Chem. Soc.* **2009**, *131*, 8376–8377.

(7) Ni, Z.; Jerrell, J. P.; Cadwallader, K. R.; Masel, R. I. *Anal. Chem.* **2007**, *79*, 1290–1293.

(8) Gu, Z. Y.; Wang, G.; Yan, X. P. *Anal. Chem.* **2010**, *82*, 1365–1370.

(9) Zhou, Y. Y.; Yan, X. P.; Kim, K. N.; Wang, S. W.; Liu, M. G. *J. Chromatogr., A* **2006**, *1116*, 172–178.

(10) Gu, Z. Y.; Chen, Y. J.; Jiang, J. Q.; Yan, X. P. *Chem. Commun.* **2011**, *47*, 4787–4789.

(11) Cui, X. Y.; Gu, Z. Y.; Jiang, D. Q.; Li, Y.; Wang, H. F.; Yan, X. P. *Anal. Chem.* **2009**, *81*, 9771–9777.

(12) Chang, N.; Gu, Z. Y.; Wang, H. F.; Yan, X. P. *Anal. Chem.* **2011**, *83*, 7094–7101.

(13) Gu, Z. Y.; Jiang, J. Q.; Yan, X. P. *Anal. Chem.* **2011**, *83*, 5093–5100.

(14) Ahmad, R.; Wong-Foy, A. G.; Matzger, A. J. *Langmuir* **2009**, *25*, 11977–11979.

(15) Kim, J.; Lee, J. E.; Lee, J.; Yu, J. H.; Kim, B. C.; An, K.; Hwang, Y.; Shin, C. H.; Park, J. G.; Kim, J.; Hyeon, T. *J. Am. Chem. Soc.* **2006**, *128*, 688–689.

(16) Zhao, W. R.; Gu, J. L.; Zhang, L. X.; Chen, H. R.; Shi, J. L. *J. Am. Chem. Soc.* **2005**, *127*, 8916–8917.

(17) Luo, Y. B.; Shi, Z. G.; Gao, Q.; Feng, Y. Q. *J. Chromatogr., A* **2011**, *1218*, 1353–1358.

(18) Li, X. S.; Wu, J. H.; Xu, L. D.; Zhao, Q.; Luo, Y. B.; Yuan, B. F.; Feng, Y. Q. *Chem. Commun.* **2011**, *47*, 9816–9818.

- (19) Lohe, M. R.; Gedrich, K.; Freudenberg, T.; Kockrick, E.; Dellmann, T.; Kaskel, S. *Chem. Commun.* **2011**, *47*, 3075–3077.
- (20) Kim, S. B.; Cai, C.; Sun, S. H.; Sweigart, D. A. *Angew. Chem., Int. Ed.* **2009**, *48*, 2907–2910.
- (21) Ke, F.; Qiu, L. G.; Yuan, Y. P.; Jiang, X.; Zhu, J. F. *J. Mater. Chem.* **2012**, *22*, 9497–9500.
- (22) Huo, S. H.; Yan, X. P. *Analyst* **2012**, *137*, 3445–3451.
- (23) Morris, W.; Doonan, C. J.; Furukawa, H.; Banerjee, R.; Yaghi, O. M. *J. Am. Chem. Soc.* **2008**, *130*, 12626–12627.
- (24) Modrow, A.; Zargarani, D.; Herges, R.; Stock, N. *Dalton Trans.* **2012**, *41*, 8690–8696.
- (25) Chui, S. S. Y.; Lo, S. M. F.; Charmant, J. P. H.; Orpen, A. G.; Williams, I. D. *Science* **1999**, *283*, 1148–1150.
- (26) Wong-Foy, A. G.; Lebel, O.; Matzger, A. J. *J. Am. Chem. Soc.* **2007**, *129*, 15740–15741.
- (27) Eddaoudi, M.; Kim, J.; Rosi, N.; Vodak, D.; Wachter, J.; O’Keeffe, M.; Yaghi, O. M. *Science* **2002**, *295*, 469–472.
- (28) Lee, E. Y.; Jang, S. Y.; Suh, M. P. *J. Am. Chem. Soc.* **2005**, *127*, 6374–6381.
- (29) Cohen, S. M. *Chem. Sci.* **2010**, *1*, 32–36.
- (30) Cohen, S. M. *Chem. Rev.* **2012**, *112*, 970–1000.
- (31) Zacher, D.; Schmid, R.; Wöll, C.; Fischer, R. A. *Angew. Chem., Int. Ed.* **2011**, *50*, 176–199.
- (32) Jung, S.; Kim, Y.; Kim, S.; Kwon, T. H.; Huh, S.; Park, S. *Chem. Commun.* **2011**, *47*, 2904–2906.
- (33) Hong, R. Y.; Pan, T. T.; Li, H. Z. *J. Magn. Magn. Mater.* **2006**, *303*, 60–68.
- (34) Tranchemontagne, D. J.; Hunt, J. R.; Yaghi, O. M. *Tetrahedron* **2008**, *64*, 8553–8557.
- (35) Buso, D.; Nairn, K. M.; Gimona, M.; Hill, A. J.; Falcaro, P. *Chem. Mater.* **2011**, *23*, 929–934.
- (36) Song, Y. B.; Gan, W. P.; Li, Q.; Guo, Y.; Zhou, J. P.; Zhang, L. N. *Carbohydr. Polym.* **2011**, *86*, 171–176.
- (37) Wang, C. M.; Zhang, H. L.; Sun, Y.; Li, H. L. *Anal. Chim. Acta* **1998**, *361*, 133–139.
- (38) Müller, M.; Turner, S.; Lebedev, O. I.; Wang, Y. M.; Tendeloo, G. V.; Fischer, R. A. *Eur. J. Inorg. Chem.* **2011**, 1876–1887.
- (39) Zhao, Y. B.; Wu, W.; Chen, J. F.; Zou, H. K.; Hu, L. L.; Chu, G. W. *Ind. Eng. Chem. Res.* **2012**, *51*, 3811–3818.
- (40) Petit, C.; Bandosz, T. J. *Adv. Funct. Mater.* **2010**, *20*, 111–118.
- (41) Cano, F. G.; Zafón, V. B.; Lucena, R.; Cárdenas, S.; Martínez, J. M. H.; Ramos, G. R.; Valcárcel, M. J. *Chromatogr., A* **2011**, *1218*, 1802–1807.
- (42) Guo, L.; Lee, H. K. *J. Chromatogr., A* **2011**, *1218*, 9321–9327.
- (43) Zhang, S. L.; Du, Z.; Li, G. K. *Anal. Chem.* **2011**, *83*, 7531–7541.
- (44) Emmenegger, C.; Kalberer, M.; Morrical, B.; Zenobi, R. *Anal. Chem.* **2003**, *75*, 4508–4513.
- (45) Zhang, Z. M.; Tan, W.; Hu, Y. L.; Li, G. K.; Zan, S. *Analyst* **2012**, *137*, 968–977.
- (46) Bhalla, K.; Singh, S. B.; Agarwal, R. *Environ. Monit. Assess.* **2010**, *167*, 515–520.
- (47) Xie, W.; Han, C.; Zheng, Z. Q.; Chen, X. M.; Qian, Y.; Ding, H. Y.; Shi, L.; Lv, C. H. *Food Chem.* **2011**, *127*, 890–892.